Description, Characterization and Assessment of a BioInspired Shoulder Joint-First Link Robot for NeuroRobotic Applications

Sardellitti, I.; Cattin, E.; Roccella, S.; Vecchi, F.; Carrozza, M.C.; Dario, P.; Artemiadis, P.K.; Kyriakopoulos, K.J.Biomedical Robotics and Biomechatronics, 2006. BioRob 2006. The First IEEE/RAS-EMBS International Conference on112-117February 20-22, 2006学术搜索

Description, Characterization and Assessment of a Bio-Inspired Shoulder Joint-First Link Robot for Neuro-Robotic Applications*

Irene Sardellitti, Emanuele Cattin, Stefano Roccella, Fabrizio Vecchi, Maria Chiara Carrozza, Paolo Dario°

ARTS and CRIM° Laboratories
Scuola Superiore Sant'Anna
v.le Piaggio 34, 56025 Pontedera, Italy
carrozza@sssup.it

Panagiotis K. Artemiadis, Kostas J. Kyriakopoulos

Control Systems Lab, Mechanical Eng. Dept.
National Technical University of Athens
9 Heroon Polytechniou Str, Athens, 157 80, Greece
{partem, kkyria}@mail.ntua.gr

Abstract **– The development of innovative exoskeletons for the upper limb requires a strong collaboration between robotics and neuroscience. The robotic system will be deeply coupled to the human user and the exoskeleton design should be based on the human model in terms of biomechanics, and control and learning strategies. This paper presents the preliminary results of the design process of the Neurobotics exoskeleton (NEUROexos). A bioinspired three joints-three links robotic arm is under development for implementing bioinspired control strategies and for obtaining a human-like robotic arm to be used for assessing active exoskeletons in fully safe conditions. In particular, this paper presents the shoulder joint-first link prototype, the selected actuation system, the actuator modelling and identification, and the experimental evaluation of the prototype capability to replicate the human shoulder kinematics during the execution of a catching task.**

Index Terms **– Robotic arm, exoskeleton, biomechanical model, neuro-rehabilitation, neuro-robotics.**

I. Introduction

An exoskeleton can be defined as an external system that is worn by human, and the physical contact between the operator and the exoskeleton allows direct transfer of mechanical power and information signals [1]. According to the results of the great research effort addressed at developing exoskeleton for neuro-rehabilitation, one of the major problem is related to the control system that has to match embedded and autonomous control (the local intelligence) with the voluntary user's intention (the high level controller): the ultimate aim is to obtain a safe and intelligent behavior under the control of the user's brain and to create a Hybrid Bionic System (HBS). The system should be able to detect the user's motor intentions, to dynamically monitor/copy movements of the limbs and to augment performance in terms of accuracy, strength, endurance, reactivity. Other fundamental requirements are: the kinematic coupling between the exoskeleton mechanical structure and the human limb, the continuous quantitative monitoring of the human limb performance while the system is worn and operated by the user, and the dynamic coupling for supporting the human limb movement by safely integrating the actuation system in parallel to the natural muscular system. These results may be obtained by investigating and implementing bio-inspired control and learning strategies, and bio-inspired mechanisms and actuation. In this specific case, bio-inspired means that the hardware and the control systems must be based on neuroscience models that synthesize neuroscience knowledge of motor control and perception and actions schemes.

In order to develop innovative exoskeletons for the upper limb, a bio-inspired design approach is being pursued [2]. The first Neurobotics exoskeleton (NEUROexos) will assist and support the human arm during the catching task of a flying object. This is a very challenging task, well known in neuroscience for investigating motor control strategies, consequently it has been chosen as a specific benchmarking performance for the first NEUROexos. The first phases of NEUROexos designing have been based on the analysis of the human biomechanics during the execution of the selected task. A biomechanical model of the upper limb for studying the human arm kinematics, dynamics, and muscolar synergies during the catching of a flying object has been experimentally and numerically defined [2]. This biomechanical model has been also used to define the specifications of the actuation system that will be coupled with the human arm. The next step is the development of a neuro-robotic arm able to replicate the human arm kinematics and dynamics during the execution of the same catching task. The object motion is planar, so a three joints-three links robotic arm actuated by six actuators in agonist/antagonist configuration has been designed. From the robotics point of view, this robotic arm will assess technical and control solutions, and it will be the bio-inspired platform that will be coupled with the first

* This work is supported by the EU within the NEUROBOTICS Integrated Project (The fusion of NEUROscience and roBOTICS, IST-FET Project #2003-001917).

prototype of actuated exoskeleton in order to implement experiments of coupled control in fully safe conditions. From the neuroscience point of view, this platform is an experimental assessment of human motor control models.

This paper presents in detail the shoulder joint-first link prototype of the neuro-robotic arm under fabrication. In particular, its mechanical structure, the analysis and characterisation of its actuation system, and the experimental comparison with the kinematic specifications extracted from the biomechanical model of the human shoulder are presented.

II. Shoulder Joint

The development of the shoulder joint-first link prototype is the first step for the development of the three joints-three links robotic arm. The joint link has the same inertial properties of the corresponding human arm segments and is driven by two hydraulic pistons placed in agonist/antagonist configuration. The hydraulic pistons are connected to the rotational joint by means of two Bowden cables. The advantage of using cables consists in the possibility to actuate remotely the joint, with a low inertia transmission system, without bulky terminal energy transformation systems. The joint is equipped with two miniature load cells series XFL225D (FGP sensors, Paris, France) to measure the forces acting on the joint exerted by the two pistons. The load cells are placed at the connection point between the sheath and the structure of the joint. This position at the end of the cable transmission allows to measure the net force transmitted at the joint. Nokon® Konkavex cable (NOKON, Süssen, Germany), a new Bowden cable type, is used to ensure the minimum force transmission loss and more lightness of the transmission. It is composed of a glass fiber reinforced teflon liner and a cable housing made of aluminum that ensures a better force transmission. A optical encoder measures the angular position of the joint. The pistons are equipped with potentiometers series 173 Analog- Output Subminiature Position Transducer (Space Age Control Inc., USA). Between the cylinder and the joint a spring is placed to ensure the safety of the system and to allow a more precise tuning of the stiffness at the joint during the co-contraction. The spring is the first arrangement to verify how the joint works and it will be substituted with a timely viscous-elastic element to ensure the desired bandwidth of the system. Moreover each piston is equipped with one pressure sensor for each chamber. Fig. 1 depicts the first prototype of the shoulder joint-first link.

The choice to actuate the joint with an agonist/antagonist configuration comes from the idea to develop a platform for experimental assessments of human control models. According to the neuroscience studies about the human sensory-motor strategies to control the limb movements, it emerged that the Central Nervous System (CNS) seems to implement an adaptive control of mechanical impedance by the co-activation of the antagonist muscles [3]. In order to replicate from a robotic point of view the human muscular co-activation, it has been chosen to develop a joint with an agonist/antagonist configuration obtained with 2n actuators, where n is the number of degrees of freedom (DoF). This actuators configuration has the disadvantage of increasing the dimension of the actuation package but makes possible an independent joint control in an agonist/antagonist way.

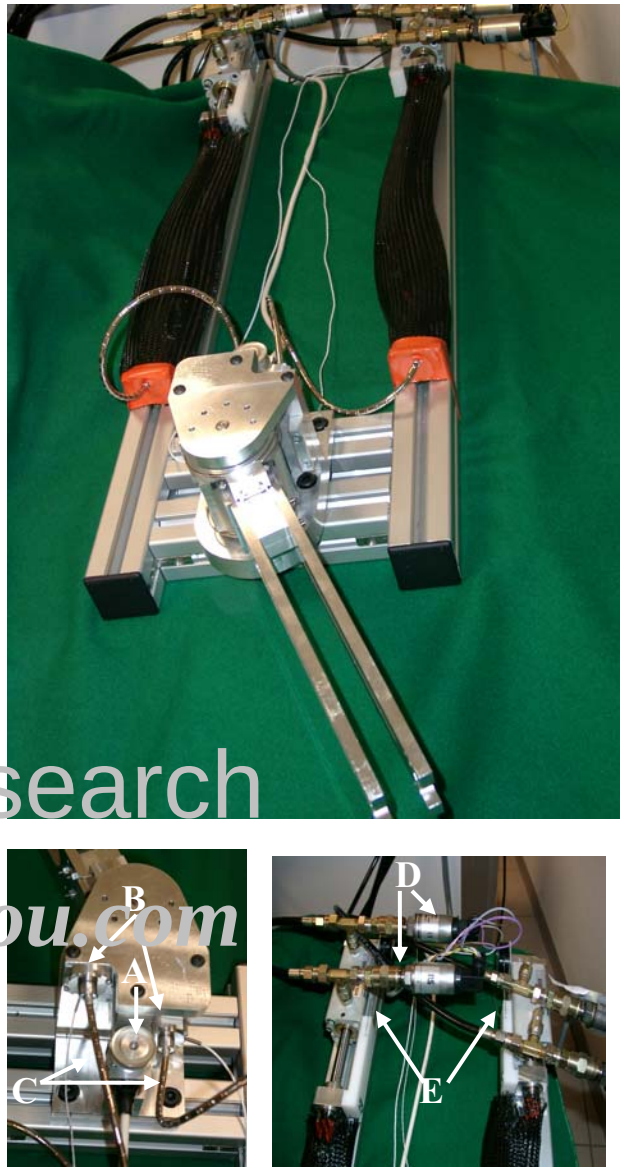

Fig 1.The shoulder joint-first link prototype: Shoulder top view (top), encoder (A), load cells (B), and Bowden cables (C) (bottom left), pressure sensors (D) and potentiometers (E) mated with the pistons (bottom right).

III. Analysis of the Actuation System

The characteristics and performances of different kind of actuators have been analyzed for selecting the actuation system of the bioinspired neuro-robotic arm [4]. In particular, this trade-off analysis has been focused on hydraulic and pneumatic actuators systems because they present the same maximum frequency of the human muscle. The hydraulic actuation has been finally selected because of its higher power/weight ratio, its higher efficiency, its capability to lift and hold heavy loads without brakes, to move heavy objects at slow speeds, to

apply torque without gearing, and its capability to generate constant pressure without significant additional energy [4],[5].

The hydraulic actuator selected for this application is shown in Fig.2. It consists of an Electric Motor (1.1 kW, 1390 rpm) an unloading valve (350 bar, 40 l/min), an accumulator (250 bar, 5.7 liters), an oiltank (30 liters), six direct-operated proportional DC valves, series D1FP*S (Parker Hannifin Corporation) and six single-rod double acting hydraulic cylinders CHL (Parker Hannifin Corporation) with a maximum pressure of 100 bar.

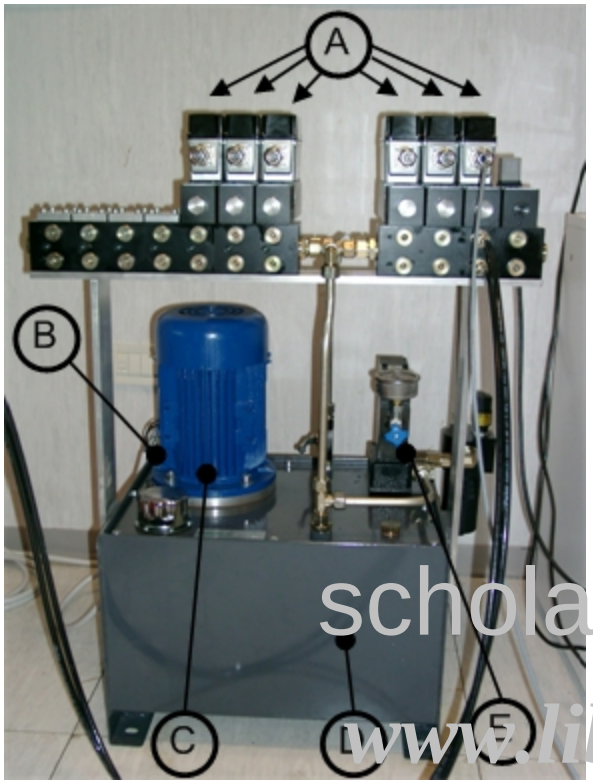

Fig. 2. Hydraulic system. A: electro-valves, B: accumulator, C: motor, D: oil tank, E: unloading valve.

By using accumulators to store energy, the hydraulic power unit only needs to provide slightly more than the average demand, increasing efficiencies for machines with varying load cycles.

Each electro-valve is characterized by three-land-four-way zero-lapped spool valve. The spool valve has a step response of 3.5 ms and its dynamic behavior does not depend on the system pressure. Moreover the electro-valves are equipped with specific electronic units for the closed loop control of the spool position. The scheme of the hydraulic actuator is shown in Fig.3.

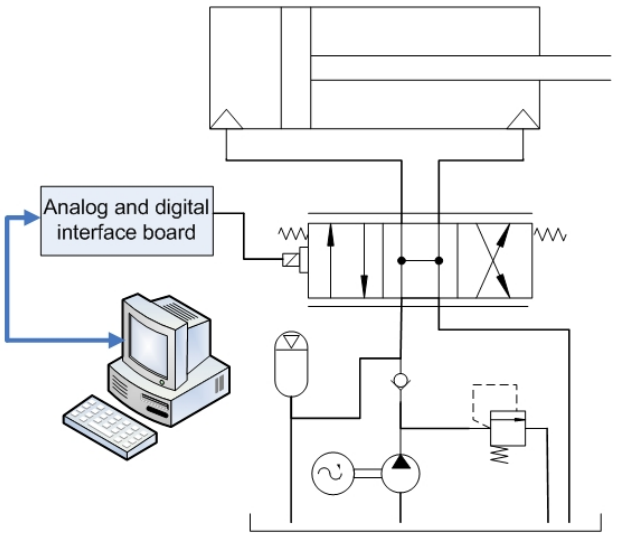

Fig. 3. Scheme of the hydraulic actuator

In particular, a solenoid associated with the electrovalve determines the up and down movements of the piston, displacing the spool valve according to the control signal (±10V). By increasing the positive input voltage sent to the electrovalve, the oil flow from the pump to the first chamber of the cylinder and pressure increases and determines the up movement of the piston with increasing velocity. In case of negative voltage, the pressure increasing in the second chamber of the cylinder determines the down movement of the piston.

A. System modeling

The agonist-antagonist system architecture is depicted in Fig. 4.

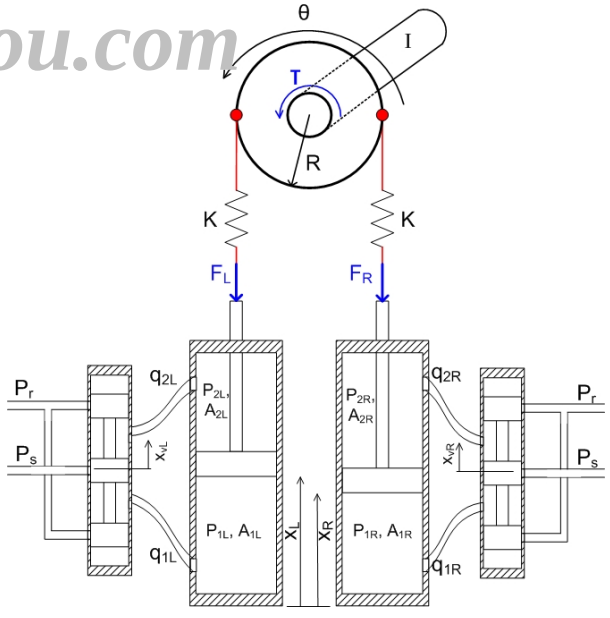

Fig. 4. Shoulder joint architecture with the agonist-antagonist actuation system.

The equation of the motion of the link is:

$$I\ddot{\vartheta} + b\dot{\vartheta} = (F_L - F_R)R \quad (1)$$

where I is the moment of inertia of the link with respect to the rotational axis of the joint, b is the friction coefficient, ϑ is the angular position, F_L, F_R are the forces exerted by the left and right piston respectively and R is the radius of the pulley. The forces F_L and F_R are given by

$$F_L = P_{1L}A_{1L} - P_{2L}A_{2L} \quad (2)$$

$$F_R = P_{1R}A_{1R} - P_{2R}A_{2R} \quad (3)$$

where P_{1L}, P_{2L}, P_{1R}, P_{2R} are the pressure values inside the chambers of the left and right piston respectively and A_{1L}, A_{2L}, A_{1R}, A_{2R} are the corresponding piston and rod side cylinder areas.

In particular for the areas there are the following relationship:

$$A_{1L} = A_{1R} = A_1 \quad (4)$$

$$A_{2L} = A_{2R} = A_2 \quad (5)$$

By considering the mathematical model of one piston the governing equation for the hydraulic cylinder displacement, disregarding external forces, is given by

$$M\ddot{x} + g(\dot{x}) = P_1A_1 - P_2A_2 \quad (6)$$

where $\dot{x}$ and $\ddot{x}$ represent the velocity and the acceleration of the piston, respectively, M the total mass being moved and $g(\dot{x})$ is the friction force.

By considering the continuity equation for the two chambers of the piston, if $\beta = V dP/dt$ is the fluid bulk modulus, and V the chamber volume, then the derivatives of the pressure in the piston chambers with respect to time, are given by the following equations:

$$\dot{P}_1 = \frac{\beta}{V_1(x)}\left(-\dot{V}_1 + Q_1\right) \quad (7)$$

$$\dot{P}_2 = \frac{\beta}{V_2(x)}\left(-\dot{V}_2 + Q_3\right) \quad (8)$$

for command signal $u \geq 0$, and

$$\dot{P}_1 = \frac{\beta}{V_1(x)}\left(-\dot{V}_1 + Q_4\right) \quad (9)$$

$$\dot{P}_2 = \frac{\beta}{V_2(x)}\left(-\dot{V}_2 + Q_2\right) \quad (10)$$

for command signal $u < 0$,

where Q_1, Q_2, Q_3, Q_4 represent the flows that came from the valve orifices and

$$V_1(x) = V_1^{(0)} + xA_1 \quad (11)$$

$$V_2(x) = V_2^{(0)} + (s - x)A_2 \quad (12)$$

where $V_1^{(0)}$ and $V_2^{(0)}$ are the initial values of the volume of the fluid trapped in the respective chambers of the piston, and *s* the stroke length of the piston.

Considering the four-way spool valve shown in Fig.3, the functioning of the valve can be visualizing as the wheaston bridge shown in Fig.5.

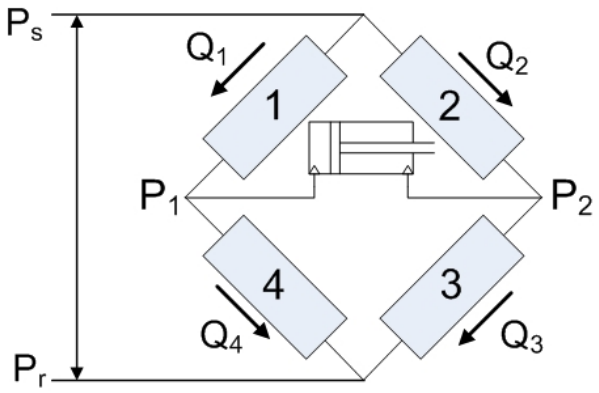

Fig. 5. Three-land-four-way spool valve

The arrows at the ports indicate the direction of the flow and the numbers at the ports indicate the orifices of the valve. Neglecting leakage in the valve, flows through the valve orifices are described by the following equations:

$$Q_1 = c_1 u\sqrt{(P_s - P_1)} \quad (13)$$

$$Q_2 = c_2 u\sqrt{(P_s - P_2)} \quad (14)$$

$$Q_3 = -c_3 u\sqrt{(P_2 - P_r)} \quad (15)$$

$$Q_4 = -c_4 u\sqrt{(P_1 - P_r)} \quad (16)$$

where P_s is the supply pressure, P_r is the reservoir pressure, and c_1, c_2, c_3, and c_4 are the valve orifice coefficients. These coefficients depend on the discharge coefficient C_d, on the density ρ of the oil and the orifice areas A that are function of the spool valve displacement x_v.

In particular

$$A_1 = A_1(x_v) \qquad A_2 = A_2(-x_v) \quad (17)$$

$$A_3 = A_3(x_v) \qquad A_4 = A_4(-x_v)$$

Regarding the valve, it can be consider as a second-order system, so the equation of motion can be given as

$$\ddot{x}_V + 2\zeta\omega\dot{x}_V + \omega^2 x_V = \omega^2 u \quad (18)$$

Because of the fact that the dynamics of the valves are much faster than those of the piston, it is assumed that the spool position is directly proportional to the command signal. By this fact it is possible to consider that the area of the orifices is a linear function of the command signal u.

B. Parameters identification

Using equations (7-10) and (13-16), the coefficients the valve orifice coefficients c_1, c_2, c_3, and c_4 have been identified:

$$c_1 = \frac{1}{u\sqrt{P_s - P_1}}\left(\frac{\dot{P}_1 V_1}{\beta} + \dot{V}_1\right) \quad (19)$$

$$c_2 = \frac{1}{u\sqrt{P_s - P_2}}\left(\frac{\dot{P}_2 V_2}{\beta} + \dot{V}_2\right) \quad (20)$$

$$c_3 = -\frac{1}{u\sqrt{P_2 - P_r}}\left(\frac{\dot{P}_2 V_2}{\beta} + \dot{V}_2\right) \quad (21)$$

$$c_4 = -\frac{1}{u\sqrt{P_1 - P_r}}\left(\frac{\dot{P}_1 V_1}{\beta} + \dot{V}_1\right) \quad (22)$$

Thus, by applying the above equations on a number of experiments using different control values, the c_i coefficients are calculated by the least square method (see Table I).

TABLE I

c_i COEFFICIENTS ESTIMATION

Coefficients	Values
c_1	0.3667e-8
c_2	0.3404e-8
c_3	0.3282e-8
c_4	0.3276e-8

Considering that the valve orifices are matched and symmetrical, it is possible to merge these 4 coefficients in one given by the mean of the four values [7].

In order to control the velocity of the single piston a characteristic voltage-velocity function has been obtained. This was accomplished by a series of experiments. During these experiments step input voltages with variable amplitude were sent to the valve and the positions of the piston were recorded with respect to time. The voltage-velocity curve obtained is shown in Fig.6.

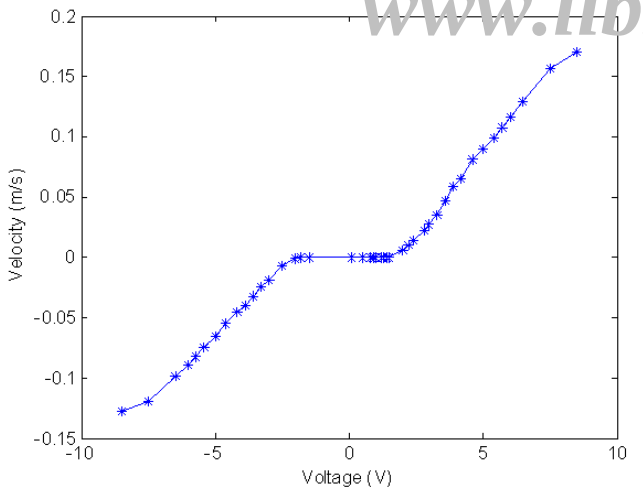

Fig. 6. Voltage-Velocity curve of a single piston.

In Fig. 6 it can be seen a dead-band zone between -1.8V and 1.5V due to the stiction of the pistons. The velocity is higher when the fluid is flowing to the piston side of the cylinder. Moreover there is a non linear area of control for high control signal values. This can occur because maximum fluid velocity is also limited by fluid viscosity and friction.

IV. Position control of the shoulder joint

A position control has been implemented on the shoulder joint prototype in order to verify the specifications of the hydraulic actuators, the performance of the agonist/antagonist configuration, and system capability to replicate the human arm kinematics during the execution of catching tasks. In order to drive the joint in an agonist/antagonist way, the developed position controller guarantees that the pistons move with the same velocity but in different directions. By moving the pistons with the same velocity, the transmission of the motion is possible because the cables are always in tense. The scheme of the implemented closed loop position control is shown in Fig. 7.

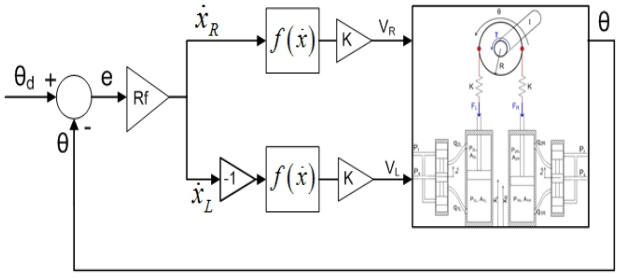

Fig. 7. Position control diagram.

ϑ_d is the desired trajectory obtained by the biomechanical model. ϑ is the actual position of the joint measured by the encoder. The desired velocity of the piston is calculated based on the error $e = \vartheta_d - \vartheta$ multiplied by the radius of the pulley R and the frequency f of the control loop. So the velocities of the pistons are given by:

$$\dot{x}_R = efR \quad (23)$$

$$\dot{x}_L = -efR \quad (24)$$

Then the command voltage signal is calculated from this velocity by considering the voltage-velocity curve shown in Fig. 6. The voltage sent to the electro-valve is obtained by

$$V_R = Kf(\dot{x}_R) \quad (25)$$

$$V_L = Kf(\dot{x}_L) \quad (26)$$

where K is the gain and $f(\dot{x}_i)$ is a function obtained based on the experimental voltage-velocity curve and that takes in account the dead-band zone showed in Fig.6.

V. EXPERIMENTAL RESULTS

The shoulder trajectory obtained from the biomechanical model during the execution of catching tasks has been used to verify the kinematic performance of the system. By considering the moment of inertia of the forearm and the hand during the catching task, a mass has been calculated and fixed on the link. The frequency of the control loop is 40 Hz. The response of the system is depicted in the Fig. 8.

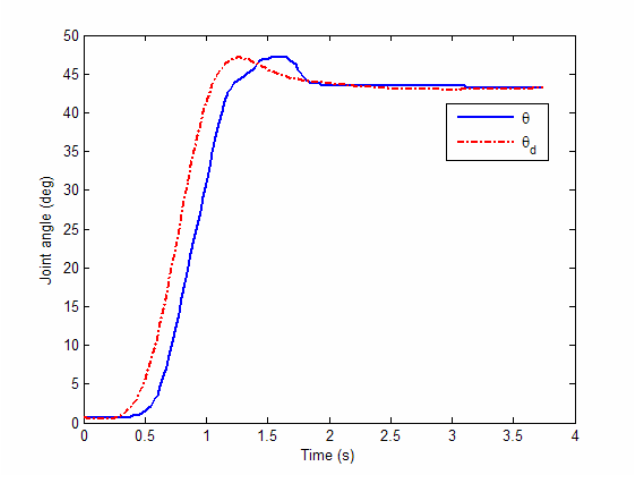

Fig. 8. Joint trajectory

As it can be seen in Fig. 8, there is a lag in the system response that causes a maximum error of 10 degrees. This lag is of 0.125 s and is mainly affected by the inertia of the system. The angular velocity profile of the joint is shown in Fig. 9.

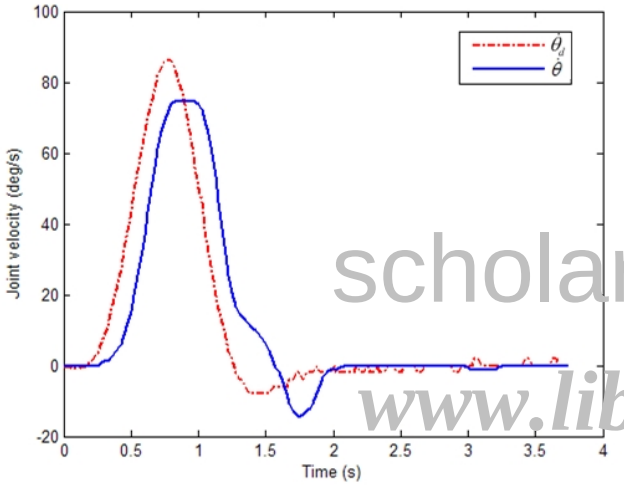

Fig. 9. Joint angular velocity

The profile of the joint velocity replicates the profile of the shoulder velocity extracted by the biomechanical model, so the system has the capability to replicate the shoulder kinematics during the execution of the catching task.

VI. Conclusions

A bioinspired robotic arm for neuro-robotic applications is being developed. This paper has presented the modeling of its hydraulic system and the shoulder joint-first link prototype. Using the model equations, a two phases parameter identification procedure has been applied. Initially, the valve orifice coefficients have been identified. The results of this phase proved that the four distinct orifice parameters can be merged to one, which is possible due to the fact that the orifices are matched and symmetrical. Then, the experimental curve relating the applied voltage and the piston velocity has been experimentally defined and approximated by mathematical formulas. A traditional position control scheme has been designed and implemented for controlling the agonist/antagonist actuator architecture. The system capability of replicating the profiles of the shoulder trajectory and velocity has been verified. The identified parameters will be used for implementing model-based control schemes that will take in account the dynamic behavior of the mechanical system. Torque and impedance controllers will be designed and implemented in order to consider the interaction of the system with the environment. Moreover, in order to experimentally verify the performance of the hydraulic system in comparison with the other drive systems, two McKibben will be implemented in agonist/antagonist configuration to drive the shoulder joint prototype for the catching task. Fig. 10 shows the concept of the three joints-three links bioinspired robotic arm under fabrication.

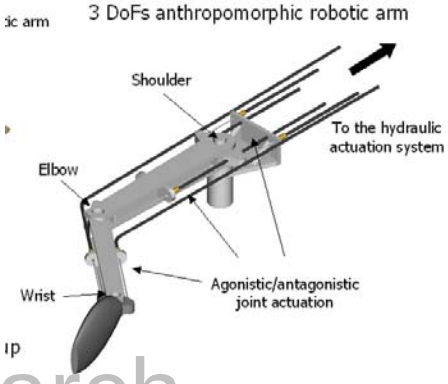

Fig. 10. Concept of 3 links-3 joint robotic arm.

The kinematic and dynamic performances of the human arm during the implementation of the catching task and of the final robotic arm will be compared using gaze-based interfaces, EMG-based interfaces, and other wearable sensory systems.

References

[1] J. Rosen, M. Brand, M. Fuchs, and M. Arcan, "A myosignal-based powered exoskeleton system systems," IEEE Trans. Syst. Man and Cybernetics, Part A, vol. 31, pp. 210–222, May 2001.

[2] M.C. Carrozza, S. Roccella, E. Cattin, F. Vecchi, P. Dario, "A Biomechanical Model of the Upper Limb for designing a Neuro-Robotic Exoskeleton", ICRA 2006, submitted.

[3] N. Hogan, "Adaptive control of Mechanical Impedance by Coactivation of Antagonist muscles," IEEE Trans. on Automatic Control, vol AC-29, 8, pp. 681- 690, August 1984.

[4] S. C. Jacobsen, H. Ko, E. K. Iversen, and C.C Davis.; "Control Strategies for Tendon.Driven Manipulators," IEEE Control Systems Magazine, pp. 23-28, February 1990.

[5] Huber, J. E.; Fleck, N. A.; Ashby, M. F., "The Selection of Mechanical Actuators Based on Performance Indices", Mathematical, Physical and Engineering Sciences, Volume 453, Issue 1965, pp. 2185-2205.

[6] Zupan M.,Ashby M.F., Fleck N.A., "Actuator classification and selection - The development of a database", Advanced Engineerings and Materials, 2002, 4, No. 12, pp.933-939.

[7] H.E. Merritt, Hydraulic control systems, John Wiley & Sons, 1967.